American Society for Microbiology | Infection and Immunity

The Phosphotransfer Protein CD1492 Represses Sporulation Initiation in *Clostridium difficile*

Kevin O. Childress,* Adrianne N. Edwards, Kathryn L. Nawrocki, Sarah E. Anderson, Emily C. Woods, Shonna M. McBride

Department of Microbiology and Immunology, Emory Antibiotic Resistance Center, Emory University School of Medicine, Atlanta, Georgia, USA

The formation of spores is critical for the survival of *Clostridium difficile* outside the host gastrointestinal tract. Persistence of *C. difficile* spores greatly contributes to the spread of *C. difficile* infection (CDI), and the resistance of spores to antimicrobials facilitates the relapse of infection. Despite the importance of sporulation to *C. difficile* pathogenesis, the molecular mechanisms controlling spore formation are not well understood. The initiation of sporulation is known to be regulated through activation of the conserved transcription factor Spo0A. Multiple regulators influence Spo0A activation in other species; however, many of these factors are not conserved in *C. difficile* and few novel factors have been identified. Here, we investigated the function of a protein, CD1492, that is annotated as a kinase and was originally proposed to promote sporulation by directly phosphorylating Spo0A. We found that deletion of *CD1492* resulted in increased sporulation, indicating that CD1492 is a negative regulator of sporulation. Accordingly, we observed increased transcription of Spo0A-dependent genes in the *CD1492* mutant. Deletion of CD1492 also resulted in decreased toxin production *in vitro* and in decreased virulence in the hamster model of CDI. Further, the *CD1492* mutant demonstrated effects on gene expression that are not associated with Spo0A activation, including lower *sigD* and *rstA* transcription, suggesting that this protein interacts with factors other than Spo0A. Altogether, the data indicate that CD1492 negatively affects sporulation and positively influences motility and virulence. These results provide further evidence that *C. difficile* sporulation is regulated differently from that of other endospore-forming species.

Clostridium difficile causes severe diarrheal infections that are difficult to treat and easily transmitted. *C. difficile* enters the host as a dormant spore, which then germinates in the presence of bile salts to form a vegetative cell (1, 2). The vegetative form of *C. difficile* then grows and divides in the host gastrointestinal tract, producing toxins that cause the symptoms of disease (3, 4). During infection, a subset of *C. difficile* vegetative cells initiates the process of sporulation and morphologically transforms into spores (5, 6). These spores are metabolically dormant and highly resistant to oxygen, heat, and chemicals that would destroy the vegetative form of *C. difficile* (7–9).

Although the signals that activate *C. difficile* sporulation have not been identified, it is expected that the master regulatory factor Spo0A must be phosphorylated for the sporulation gene expression program to begin (10–12). Once phosphorylated, active Spo0A binds DNA, promoting the expression of early sporulation-specific genes and initiating spore formation (10, 13). In the extensively studied spore former *Bacillus subtilis*, activation of Spo0A is accomplished through a phosphorelay that is composed of sensor histidine kinases and a series of phosphotransfer proteins that tightly control the phosphorylation state of Spo0A (14, 15). The *C. difficile* genome does not encode an apparent phosphorelay but does contain three putative sensor histidine kinase proteins that are anticipated to directly phosphorylate and activate Spo0A (11, 16). One of these histidine kinase proteins, CD2492, was shown to positively affect *C. difficile* sporulation, and another, CD1579, was shown to interact directly with and transfer phosphate to Spo0A *in vitro* (11). The function of the third putative sporulation histidine kinase, CD1492, is not known.

In this study, we investigated the role of the putative sporulation kinase CD1492 in *C. difficile* sporulation. We examined the sporulation-specific gene expression and resulting phenotypes of a *CD1492* deletion mutant and strains overexpressing wild-type or mutated *CD1492* alleles. Our results indicate that CD1492 is involved in the initiation of sporulation, but contrary to its proposed function, this protein plays a role in preventing spore formation. In addition, we found that the *CD1492* null mutant exhibited changes in gene expression that are not directly dependent on Spo0A activation or sporulation, including decreased production of TcdA and motility regulators. Furthermore, the *CD1492* mutant was significantly less virulent in a hamster model of infection.

MATERIALS AND METHODS

Cultivation of bacteria. *C. difficile* cultures were grown in an anaerobic chamber (Coy Laboratory Products) containing an atmosphere of 85% nitrogen, 10% hydrogen, and 5% CO_2 at 37°C as described previously (17). *C. difficile* strains were cultured in brain heart infusion (BHI) medium supplemented with 2% yeast extract (BHIS medium) as broth or 1.5% agar medium (18). *Escherichia coli* were grown at 37°C in L broth (19) or agar plates or in BHIS medium supplemented with 20 μg/ml chloramphenicol or 100 μg/ml ampicillin as needed. Thiamphenicol (2 to 10 μg/ml) was used for selection of *C. difficile* plasmids, and kanamycin (50 μg/ml) was utilized for counterselection against *E. coli* as previously

Received 22 August 2016 Accepted 12 September 2016

Accepted manuscript posted online 19 September 2016

Citation Childress KO, Edwards AN, Nawrocki KL, Anderson SE, Woods EC, McBride SM. 2016. The phosphotransfer protein CD1492 represses sporulation initiation in *Clostridium difficile*. Infect Immun 84:3434–3444. doi:10.1128/IAI.00735-16.

Editor: V. B. Young, University of Michigan

Address correspondence to Shonna M. McBride, shonna.mcbride@emory.edu.

* Present address: Kevin O. Childress, Department of Pathology, Microbiology, and Immunology, Vanderbilt University School of Medicine, Nashville, Tennessee, USA.

K.O.C. and A.N.E. contributed equally to this work.

Supplemental material for this article may be found at http://dx.doi.org/10.1128/IAI.00735-16.

TABLE 1 Bacterial strains and plasmids used in this study

Strain or plasmid	Relevant genotype or features	Source, construction, and/or reference
E. coli strains		
HB101	F^- *mcrB mrr hsdS20* (r_B^- m_B^-) *recA13 leuB6 ara-14 proA2 lacY1 galK2 xyl-5 mtl-1 rpsL20*	B. Dupuy
MC277	HB101 containing pRK24 and pMC211	28
MC527	HB101 containing pRK24 and pMC381	This study
MC559	HB101 containing pRK24 and pMC386	This study
MC779	HB101 containing pRK24 and pMC539	This study
C. difficile strains		
630	Clinical isolate	65
630Δ*erm*	Erm^s derivative of strain 630	N. Minton, 66
MC282	630Δ*erm* pMC211	28
MC587	630Δ*erm* pMC386	This study
MC674	630Δ*erm* Δ*CD1492*	This study
MC729	630Δ*erm* Δ*CD1492* pMC211	This study
MC730	630Δ*erm* Δ*CD1492* pMC386	This study
MC771	630Δ*erm* Δ*CD1492* pMC539	This study
Plasmids		
pRK24	Tra^+ Mob^+ *bla tet*	67
pUC19	Cloning vector, *bla*	68
pMTL-SC7315	For allelic exchange in nonepidemic *C. difficile* strains	N. Minton, 26
pMC123	*E. coli-C. difficile* shuttle vector, *bla catP*	69
pMC211	pMC123 P*cprA*	28
pMC381	pMTL7315 Δ*CD1492* cassette	This study
pMC386	pMC211 with *CD1492*	This study
pMC538	pUC19 *CD1492* H668A	This study
pMC539	pMC211 with *CD1492* H668A	This study

detailed (20–22). Taurocholate (Sigma-Aldrich) was added to cultures at 0.1% to induce spore germination (23).

Strain and plasmid construction. The plasmids and bacterial strains used in this study are listed in Table 1, and the details of vector constructions are outlined in File S1 in the supplemental material. Primer design was based on the *C. difficile* strain 630 genomic sequence (GenBank accession no. NC_009089.1), and the 630Δ*erm* derivative was used for PCR amplification and cloning (Table 2). Plasmid DNA isolation, PCR, and cloning were performed by using standard protocols. Plasmid sequences were verified prior to use (Eurofins MWG Operon). *C. difficile* genomic DNA was isolated as previously described (24, 25). *C. difficile-E. coli* conjugations and gene deletions were carried out as previously described (22, 23, 26).

Single nucleotide polymorphism (SNP) analysis. *C. difficile* genomic DNA was prepared as previously described (24, 25). Genomic DNA was quantitated with a NanoDrop (Thermo Scientific), and 1 ng of DNA was used for library preparation. Libraries were generated with the Nextera XT DNA Library Preparation kit (Illumina); dual barcoding and sequencing primers were added according to the manufacturer's protocol. Libraries were validated by microelectrophoresis, quantified, pooled, and clustered on an Illumina MiSeq instrument in 150-bp reads. Per-sample reads were mapped to the *C. difficile* 630 reference genome (GenBank no. AM180355). All variant analysis was performed and annotated with CLC Genomics Workbench v9.0, with the "Fixed Ploidy Variant Detection" and "Annotate with Overlap Information" tools.

Sporulation efficiency assays and phase-contrast microscopy. *C. difficile* cultures were started in BHIS medium supplemented with 0.1% taurocholate to allow for germination of spores within the starting inoculum and 0.2% fructose to prevent sporulation. When cultures reached an optical density at 600 nm (OD_{600}) of 0.5, 250 μl was applied evenly to 70:30 agar medium and incubated anaerobically at 37°C (27). Samples were scraped from the plates at the time points indicated for each experiment and evaluated for sporulation frequency by both phase-contrast counting and enumeration of ethanol-resistant spores. Samples for phase-contrast microscopy were resuspended in BHIS broth and applied to slides as previously described (28). Phase-contrast microscopy was performed with a Nikon Eclipse Ci-L microscope with an X100 Ph3 oil immersion objective, and images were acquired with a DS-Fi2 camera. Two or more fields of view were captured for each strain, and at least 1,000 cells were assessed and enumerated per experiment. The percentage of spores present was calculated as the number of spores divided by the total number of cells. The mean percentage of spores and the standard error of the mean were calculated from at least three independent experiments (24).

To determine the number of viable spores in the total viable population, *C. difficile* cultures were grown on 70:30 sporulation agar as described above and ethanol resistance assays were performed. After 24 h of growth, cells were resuspended in BHIS medium to an OD_{600} of 1.0, serially diluted in BHIS medium, and plated onto BHIS agar medium to enumerate vegetative cells. A 0.5-ml aliquot of culture was then mixed with 95% ethanol and water to a final concentration of 28.5%. Ethanol-treated cells were vortexed, incubated at room temperature for 15 min, serially diluted in 1× phosphate-buffered saline containing 0.1% taurocholate, and then plated onto BHIS medium plates containing 0.1% taurocholate to enumerate spore outgrowth. Plates were incubated for a minimum of 24 h, and the number of CFU per milliliter of starting culture was calculated. The sporulation frequency was calculated as the number of ethanol-resistant spores divided by the total number of cells (combined counts of spores and vegetative cells per milliliter). A *spo0A* mutant (MC310) was used as a control to ensure vegetative cell death in ethanol.

qRT-PCR. *C. difficile* cultures were harvested from 70:30 sporulation agar, resuspended in a cold solution of 1.5:1.5:3 ethanol-acetone-distilled H_2O, and stored immediately at −80°C. RNA was purified from the cell cultures, and cDNA was synthesized as described previously (28, 29). A 50- or 200-ng sample of cDNA was used per reaction mixture for standard

TABLE 2 Oligonucleotides used in this study

Primer	Sequence (5′→3′)	Use and/or source
oMC44	5′-CTAGCTGCTCCTATGTCTCACATC-3′	69
oMC45	5′-CCAGTCTCTCCTGGATCAACTA-3′	69
oMC112	5′-GGCAAATGTAAGATTTCGTACTCA-3′	*tcdB* (*CD0660*) qPCR, 28
oMC113	5′-TCGACTACAGTATTCTCTGAC-3′	*tcdB* (*CD0660*) qPCR, 28
oMC189	5′-TGCCTCTTGTAAAGAGTATAGCA-3′	*sigD* (*CD0266*) qPCR, 24
oMC190	5′-GCATCAATCAATCCAATGACTCCAC-3′	*sigD* (*CD0266*) qPCR, 24
oMC331	5′-CTCAAAGCGCAATAAATCTAGGAGC-3′	*spo0A* (*CD1214*) qPCR, 28
oMC332	5′-TTGAGTCTCTTGAACTGGTCTAGG-3′	*spo0A* (*CD1214*) qPCR, 28
oMC333	5′-AGTAAGGGTATGGGCAAAGTATTACA-3′	*CD1579* qPCR, 24
oMC334	5′-CCACTTCATTTGAGAACAACTCTTTG-3′	*CD1579* qPCR, 24
oMC335	5′-ACTTGTAAGAAGTGCTGAAGGTGGTA-3′	*CD1492* qPCR, 24
oMC336	5′-GTCATATCGACCAAATCACTTGAAACAC-3′	*CD1492* qPCR, 24
oMC337	5′-CAGGAATTTGTGACTATCTGGGAAATGG-3′	*CD2492* qPCR, 24
oMC338	5′-TCCCATTTGCCTTTATTTGAACTTGA-3′	*CD2492* qPCR, 24
oMC339	5′-GGGCAAATATACTTCCTCCTCCAT-3′	*sigE* (*CD2643*) qPCR, 28
oMC340	5′-TGACTTTACACTTTCATCTGTTTCTAGC-3′	*sigE* (*CD2643*) qPCR, 28
oMC355	5′-CTGTTGGAATATCTAGGCGATAAGC-3′	*rstA* (*CD3668*) qPCR, 24
oMC356	5′-TGGTCCTCAGCCTTGTTTAATTC-3′	*rstA* (*CD3668*) qPCR, 24
oMC365	5′-GGAAGTAACTGTTGCCAGAGAAGA-3′	*sigF* (*CD0772*) qPCR, 28
oMC366	5′-CGCTCCTAACTAGACCTAAATTGC-3′	*sigF* (*CD0772*) qPCR, 28
oMC547	5′-TGGATAGGTGGAGAAGTCAGT-3′	*tcdA* qPCR (*CD0663*), 28
oMC548	5′-GCTGTAATGCTTCAGTGGTAGA-3′	*tcdA* qPCR (*CD0663*), 28
oMC569/tcdRqF	5′-AGCAAGAAATAACTCAGTAGATGATT-3′	*tcdR* qPCR (*CD0659*), 40
oMC570/tcdRqR	5′-TTATTAAATCTGTTTCTCCCTCTTCA-3′	*tcdR* qPCR (*CD0659*), 40
oMC897	5′-GCCATGGATCCTTGGAAGAATTGTGGTAACATATTTATAG-3′	*CD1492* cloning
oMC898	5′-GATGCCTGCAGACGCATCAAATACAACTAAAGTAATAAA-3′	*CD1492* cloning
oMC911	5′-GCGCGGCCGCGAGTAGGAAATCTGGCTTAT-3′	*CD1492* deletion construct
oMC912	5′-ACAACTAAAGCACTTCTTCATTTTTATATAGTTTTACC-3′	*CD1492* deletion construct
oMC913	5′-TGAAGAAGTGCTTTAGTTGTATTTGATGCGTTTTA-3′	*CD1492* deletion construct
oMC914	5′-GCGCGGCCGCCAGCCTTGTCATTTTTTAGATTG-3′	*CD1492* deletion construct
fliCqF	5′-TACAAGTTGGAGCAAGTTATGGAAC-3′	40
fliCqR	5′-GTTGTTATACCAGCTGAAGCCATTA-3′	40

or cecal quantitative PCR (qPCR) analysis, respectively. Quantitative reverse transcription-PCR (qRT-PCR) analysis was performed with the Bioline SensiFAST SYBR and Fluorescein kit and a Roche LightCycler 96 instrument. Reaction mixtures without reverse transcriptase were included for each primer set to detect genomic DNA contamination. qPCR primers were designed with the IDT PrimerQuest program (Table 2). qPCR was performed in technical triplicate for each cDNA sample and primer pair combination. Primer efficiencies were calculated for each primer set prior to assays. Results were calculated by the comparative cycle threshold method, normalized to the internal control transcript *rpoC* (30). At least four biological replicates were assessed. Relative-expression results are presented as the means and standard errors of the means. The two-tailed Student *t* test was performed to assess the statistical significance of differences between the expression ratios of the control and test groups.

Animal studies. Spores were prepared and enumerated for animal experiments as previously described (28). Female Syrian golden hamsters (*Mesocricetus auratus*) weighing 70 to 110 g were obtained from Charles River Laboratories and maintained in an animal biosafety level 2 room within the Division of Animal Resources at Emory University. Animals were housed individually and provided standard rodent chow and water *ad libitum*. Hamsters were administered a single dose of clindamycin (30 mg/kg of body weight) by oral gavage 7 days prior to infection (day −7). At day 0, hamsters were administered approximately 5,000 spores of a single *C. difficile* strain and monitored several times per day for display of disease symptoms (weight loss, lethargy, diarrhea, or a wet tail). All animals were weighed at least once per day, and fecal samples were collected daily for determination of the total number of cells throughout the experiment. Experiments were performed two times with cohorts of five or six animals per *C. difficile* strain tested. Additional animals that received clindamycin but were not administered *C. difficile* served as negative controls in each experiment. Animals were considered moribund and were euthanized if (i) they lost 15% or more of their body weight or (ii) if they exhibited diarrhea and lethargy. Hamsters were euthanized by CO_2 asphyxiation followed by a thoracotomy. Following euthanasia, animals were necropsied and cecal contents were collected for enumeration of *C. difficile* bacteria and RNA isolation. Cecal samples used for RNA isolation were stored in 1:1 ethanol-acetone at −80°C. Strain-specific differences in the numbers of *C. difficile* CFU recovered from feces and cecal contents were determined by single-factor analysis of variance (ANOVA; GraphPad Prism 6) and by two-tailed Student *t* test (Excel; Microsoft). Differences in hamster survival for animals infected with MC674 (*CD1492*) or 630Δ*erm* were assessed with the log rank test (GraphPad Prism 6).

SDS-PAGE and Western blot analysis. *C. difficile* strains 630Δ*erm*, MC674 (*CD1492*), MC282 (630Δ*erm* P*cpr*), MC729 (*CD1492* P*cpr*), MC730 (*CD1492* P*cpr*::*CD1492*), and MC771 (*CD1492* P*cpr*::*CD1492* H668A) were grown in TY medium for 24 h at 37°C as previously described (24), except that strains were cultivated in BHIS medium overnight. Total protein was quantitated with the Pierce Micro BCA Protein Assay kit (Thermo Scientific), and 8 μg of total protein was loaded onto precast TGX 4 to 15% gradient gels (Bio-Rad), separated by electrophoresis, and subsequently transferred to 0.45-μm nitrocellulose membranes (Bio-Rad). Western blot analysis was conducted with mouse anti-TcdA antibodies (Novus Biologicals), followed by a goat anti-mouse Alexa Fluor 488 secondary antibody (Life Technologies). Imaging and densitometry were performed with a ChemiDoc and Image Lab Software (Bio-Rad), and three biological replicates were analyzed for each strain. The

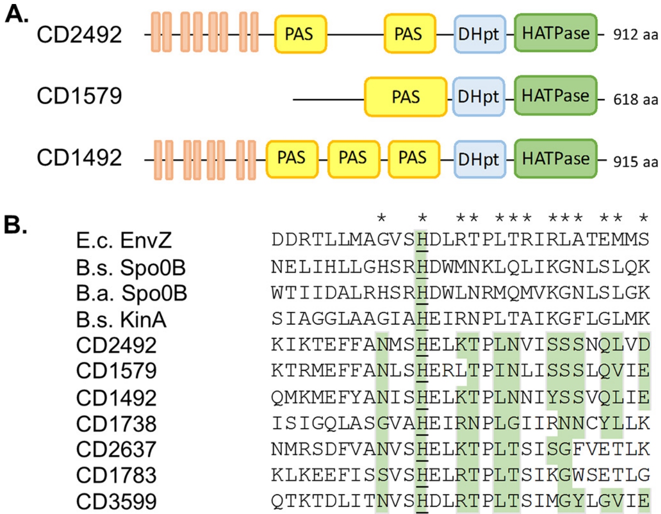

FIG 1 *In silico* analysis of sporulation-associated histidine kinases. (A) Tan boxes represent predicted transmembrane domains; the H^+ ATPase region includes the kinase catalytic domain (56, 57). DHpt, dimerization and histidine phosphotransferase; aa, amino acids. (B) Alignment of the dimerization and histidine phosphotransfer subdomains of *C. difficile*, *B. subtilis*, and *B. anthracis* sporulation kinases and *E. coli* EnvZ. The known or suspected conserved histidine is underlined. Asterisks represent the residues involved in direct interactions with the cognate response regulators (11, 61, 62), and shaded residues are highly conserved in *C. difficile*. E.c., *E. coli*; B.s., *B. subtilis*; B.a., *Bacillus anthracis*.

Student two-tailed *t* test and a one-way ANOVA, followed by Dunnett's multiple-comparison test, were performed to assess statistical differences in TcdA protein levels between the mutant and parent strains and the complemented strains, respectively (GraphPad Prism 6). A representative Western blot image is shown.

Motility studies. Strains were grown in BHIS medium to an OD_{600} of 0.5, and 5 μl of culture was spotted into the center of one-half-concentration BHI plates containing 0.3% agar. Swimming diameters were measured every 24 h for a total of 168 h. Results represent the mean values and the standard errors of the means for a minimum of three independent experiments. A two-tailed Student *t* test was performed to determine statistically significant differences in outcomes between the mutant and parent strains.

RESULTS

Deletion of the predicted orphan kinase gene *CD1492* results in increased spore formation. The genome of *C. difficile* strain 630 encodes three putative orphan histidine kinases that have been implicated as sporulation sensor kinases: CD1492, CD1579, and CD2492 (11). Previous investigations found that disruption of the CD2492 kinase results in a significant decrease in spore formation, while the CD1579 kinase was shown to affect Spo0A phosphorylation *in vitro* (11). CD1492, the third suspected sporulation sensor kinase, has not been directly linked to a sporulation phenotype or phosphorylation of Spo0A *in vitro*. As outlined in Fig. 1, CD1492 and CD2492 both have multiple predicted transmembrane segments, while CD1579 is an apparent cytosolic protein. All three proteins have predicted histidine kinase catalytic domains of typical sensor histidine kinases.

To investigate the potential influence of CD1492 on sporulation, we deleted the coding sequence by double crossover by markerless allelic exchange (see Fig. S2 in the supplemental material) (26). Expression of *CD1492* in the *CD1492* null mutant MC674 was ablated, as expected, and no growth defect was observed in any medium tested (data not shown). Whole-genome SNP analysis by Illumina next-generation sequencing revealed no additional nucleotide changes in the *CD1492* mutant (see Materials and Methods). The *CD1492* mutant was tested for the ability to sporulate on 70:30 sporulation agar (27). As demonstrated in Fig. 2A and Table 3, the *CD1492* mutant produced significantly more spores than the parent strain, having a sporulation frequency approximately 2.4-fold higher than that of the parent strain, as determined by phase-contrast microscopy (630Δ*erm*, 23.4% ± 5.1%; MC674, 56.4% ± 6.8%). Similarly, the production of ethanol-resistant spores was 3.4-fold higher for the *CD1492* mutant than for the parent strain (Fig. 2B; 630Δ*erm*, 23.0% ± 8.0%; MC674, 79.1% ± 5.3%), demonstrating that the spores produced by the mutant are fully formed and viable. The high-spore-forming phenotype of the *CD1492* mutant suggests that, unlike many other sporulation histidine kinases, CD1492 is a negative regulator of sporulation initiation. On the basis of the mutant phenotype, CD1492 is unlikely to function solely as a sporulation sensor kinase that activates Spo0A by phosphorylation, as was predicted through *in silico* analyses. Alternatively, CD1492 may act as a phosphatase that inactivates Spo0A to prevent sporulation or it may activate a sporulation-repressing function.

The *CD1492* mutant has elevated sporulation-specific gene expression. To determine the effect of the *CD1492* mutation on sporulation initiation, the abundance of key early sporulation

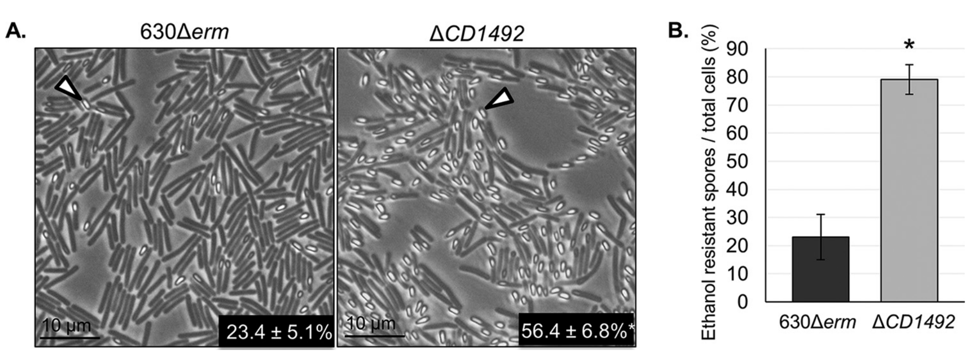

FIG 2 The Δ*CD1492* mutant has a hypersporulation phenotype. (A) Representative phase-contrast micrographs of the parent strain (630Δ*erm*) and the Δ*CD1492* mutant (MC674) grown on 70:30 sporulation agar for 24 h. Open arrowheads indicate phase-bright spores. (B) Ethanol-resistant spore formation frequency per total viable cells of the 630Δ*erm* and Δ*CD1492* mutant strains collected from 70:30 sporulation agar after 24 h. Sporulation frequencies were calculated as described for each assay in Materials and Methods. The mean values and the standard errors of the means are shown. *, $P \leq 0.05$ by a two-tailed Student *t* test.

TABLE 3 The *C. difficile CD1492* mutant forms more ethanol-resistant spores on 70:30 sporulation agar

Strain	No. of CFU/ml			Sporulation frequency[d]	% Sporulation
	Vegetative cells[a]	Spores[b]	Total cells[c]		
630Δ*erm*	$1.49 \times 10^8 \pm 2.13 \times 10^7$[e]	$3.60 \times 10^7 \pm 6.18 \times 10^6$	$1.85 \times 10^8 \pm 1.61 \times 10^7$	$2.23 \times 10^{-1} \pm 7.28 \times 10^{-2}$	22.3 ± 7.28
Δ*CD1492*	$1.64 \times 10^7 \pm 3.88 \times 10^6$	$5.33 \times 10^7 \pm 5.98 \times 10^6$	$6.97 \times 10^7 \pm 8.03 \times 10^6$	$7.76 \times 10^{-1} \pm 5.18 \times 10^{-2}$	77.6 ± 5.18

[a] The numbers of vegetative cells are the numbers of CFU recovered on BHIS medium plates.
[b] The number of spores is the total number of CFU that survived ethanol treatment as described in Materials and Methods and were recovered on BHIS medium plates supplemented with 0.1% taurocholate.
[c] The total cell numbers include both vegetative cells and spores.
[d] The sporulation frequency was calculated as the number of ethanol-resistant spores divided by the total number of cells.
[e] Values are means and standard errors of the means.

transcripts, relative to the parent strain, was measured during growth on sporulation medium. Transcription of the master sporulation regulator *spo0A* was slightly higher in the *CD1492* mutant after 12 h on sporulation medium, but this difference did not reach statistical significance (Fig. 3A). Further, the transcription of the Spo0A-dependent sigma factors *sigF* and *sigE* was >2-fold higher in the *CD1492* mutant strain ($P \leq 0.05$). SigF and SigE are required for forespore and mother cell-specific sporulation gene expression, respectively (31). The greater sporulation frequencies and higher early sporulation gene expression of the *CD1492* mutant suggest that a greater proportion of these cells enters the sporulation pathway.

As mentioned previously, CD1492 is one of three orphan kinases that are proposed to function as sporulation sensor kinases. We found that expression of one of the suspected sporulation kinases, *CD1579*, was 2-fold lower in the *CD1492* mutant, while expression of *CD2492* was similar to that in the parent strain (Fig. 3B). Thus, CD1492 has a modest effect on the expression of one of the other suspected kinases.

In the model spore former *B. subtilis*, the sporulation sensor kinases facilitate sporulation initiation through the sporulation phosphorelay, which consists of the intermediate proteins Spo0F and Spo0B that enable phosphotransfer to Spo0A (32). As initiators of sporulation, the *B. subtilis* kinases are expressed prior to the onset of sporulation and their expression wanes in a sporulating population as sporulation progresses (32). We investigated the expression of *CD1492* during growth on sporulation medium to determine how the timing of its transcription relates to sporulation initiation. Samples of the parent strain were taken during growth on 70:30 medium and assessed for *CD1492* and *sigE* expression over time (see Fig. S3 in the supplemental material). Relative to transcription at 6 h after transfer to sporulation medium (H_6, logarithmic phase), the transcription of *CD1492* increased about 5-fold at 8 h postinoculation (H_8). *CD1492* transcript levels declined at later time points, even as levels of the early mother cell sigma factor *sigE* remained elevated. The decline in *CD1492* expression during early sporulation implies that CD1492 is involved prior to the initiation of sporulation. The hypersporulation phenotype of the *CD1492* mutant and the timing of *CD1492* expression suggest that CD1492 acts as a negative regulator of sporulation before initiation.

A conserved catalytic histidine residue is required for CD1492 function. To confirm that the *CD1492* deletion was responsible for the mutant phenotypes, complementation was performed with a wild-type *CD1492* allele under the control of the nisin-inducible *cprA* promoter (20, 28). As illustrated in Fig. 4, complementation of the *CD1492* mutant with an inducible *CD1492* allele (*CD1492* pP*cprA*::*CD1492*, MC730) resulted in reduced spore formation. The restoration of the parental sporulation phenotype in the complemented strain demonstrates that the *CD1492* mutation is responsible for the increased sporulation frequency of the mutant and suggests that the timing of *CD1492*

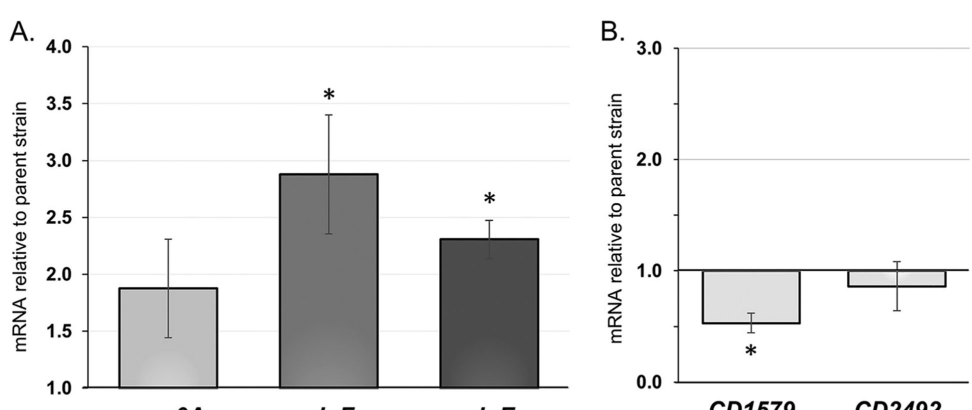

FIG 3 Expression of key early sporulation regulators and putative sporulation kinases in the Δ*CD1492* mutant. Transcriptional analysis of *spo0A*, *sigF*, and *sigE* (A) and predicted sporulation kinase CD1579 and CD2492 expression (B) in the Δ*CD1492* mutant (MC674) relative to that in parent strain 630Δ*erm*. Cultures were grown on 70:30 sporulation agar for 12 h, RNA was harvested, cDNA was prepared, and qRT-PCR was performed with gene-specific primers as outlined in Materials and Methods. The mean values and the standard errors of the means of at least three biological replicates are shown. *, $P \leq 0.05$ by two-tailed Student *t* test.

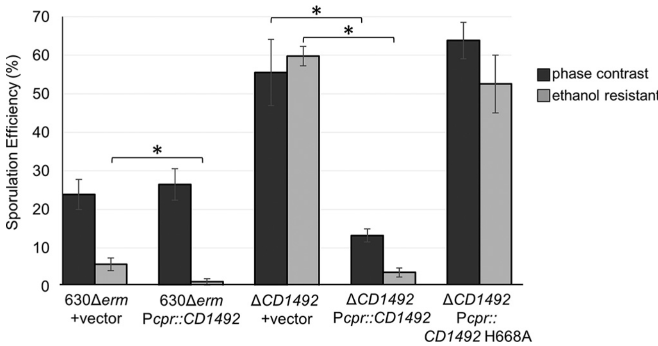

FIG 4 Complementation of Δ*CD1492* and site-directed mutagenesis of conserved sensor kinase residues. Sporulation frequencies calculated from the ratios of spores to vegetative cells by phase-contrast micrographs obtained at H_{24} (black bars) or from cells before and after treatment with ethanol (gray bars). Strains 630Δ*erm* p*Pcpr* (MC282, vector control), 630Δ*erm* p*PcprA*::*CD1492* (MC587), Δ*CD1492* p*Pcpr* (MC729, vector control), Δ*CD1492* p*PcprA*::*CD1492* (MC730), and Δ*CD1492* p*PcprA*::*CD1492*-H668A (MC771) were grown on 70:30 sporulation agar plates supplemented with 2 μg ml^{-1} thiamphenicol and 1 μg ml^{-1} nisin, and sporulation frequency assays were performed as described in Materials and Methods. The mean values and the standard errors of the means of at least four biological replicates are shown. *, $P \leq 0.05$ by two-tailed Student *t* test.

expression is not critical to its function as a negative sporulation regulator (Fig. 4; see Fig. S3 and S4 in the supplemental material). In addition, expression of exogenous CD1492 in the parent strain (630Δ*erm* p*PcprA*::*CD1492*, MC587, Fig. 4) decreased the number of ethanol-resistant spores formed, suggesting that overexpression of CD1492 can reduce sporulation in an otherwise wild-type strain. This is similar to the sporulation sensor kinases of *Bacillus* and *Clostridium* species that can affect sporulation when overexpressed (33–35). To determine if CD1492 functions as a predicted sensor histidine kinase, we created a site-directed mutation at the conserved histidine residue, substituting an alanine (H668A). Histidine-to-alanine substitutions in the conserved histidine catalytic residues of sensor kinases result in an inability of the protein to transfer phosphate signals, thereby rendering them nonfunctional (15, 36). When the *CD1492* H668A mutated allele was used to complement the *CD1492* mutant (*CD1492* p*PcprA*::*CD1492*-H668A, MC771), the sporulation frequency did not decrease relative to that of the mutant (Fig. 4). The inability of the *CD1492* H668A allele to restore the mutant phenotype strongly suggests that the phosphotransfer capability of CD1492 is essential to its function as an inhibitor of sporulation.

Deletion of *CD1492* results in decreased virulence in an animal model of infection. Although the *CD1492* mutant exhibits a higher sporulation frequency *in vitro*, the function of CD1492 in sporulation in the intestine and the effect of CD1492 on pathogenesis are not known. To this end, we examined the *CD1492* mutant in a hamster model of *C. difficile* infection. Female Syrian golden hamsters were infected by oral gavage with approximately 5,000 spores of either the *CD1492* mutant or parent strain 630Δ*erm*. Following inoculation, animals were monitored for disease symptoms and fecal samples were acquired every 24 h postinfection for enumeration of *C. difficile* bacteria. As shown in Fig. 5A, hamsters infected with *CD1492* mutant spores became moribund much more slowly than animals infected with the parent strain (mean times to morbidity: 630Δ*erm*, 45.5 ± 3.5 h; Δ*CD1492*, 107.9 ± 52.5 h; $P < 0.01$, log rank test). Determination of the total number of *C. difficile* bacteria shed in the feces of infected animals revealed no significant differences between the CFU counts of the *CD1492* mutant and parent strain infections, indicating that the mutant strain does not have an observable growth defect *in vivo* (Fig. 5B). Likewise, *C. difficile* CFU counts were similar in the cecal contents of *CD1492* mutant and parent strain-infected animals postmortem (Fig. 5C). These data indicate that the decreased virulence observed in *CD1492* mutant infections was not caused by *in vivo* defects in the outgrowth of spores or vegetative cells.

The *CD1492* mutant produces less TcdA and has lower expression of toxin-associated regulators and motility genes. On the basis of the decreased virulence and lack of a growth defect of the *CD1492* strain *in vivo*, we hypothesized that this mutant may have lower expression of the two major virulence factors toxins TcdA and TcdB (3). To investigate the impact of CD1492 on toxin production, we analyzed the expression of toxin *in vitro* and *in vivo*. The expression of *tcdA* was 2-fold lower in *CD1492* mutant cultures grown on sporulation agar (Fig. 6A), but no change in *tcdB* expression was observed. Supporting these results, a similar decrease in TcdA production was detected in strains that did not have a functional *CD1492* gene by Western blotting of *in vitro* cultures with anti-TcdA antibody (Fig. 6B). Examination of toxin transcripts from the cecal contents of animals that succumbed to infection revealed considerable variability in *tcdB* transcript production in *CD1492* mutant-infected animals, but differences in toxin expression did not achieve statistical significance (Fig. 6C).

Although the *CD1492* mutant produces less *tcdA* transcript *in vitro*, it is unlikely that CD1492 is a direct regulator of toxin transcription. Toxin expression in *C. difficile* is affected by multiple regulatory factors that integrate complex cellular nutritional signals to control nutrient acquisition and motility (37). TcdA and TcdB are directly transcribed by the toxin-specific sigma factor TcdR, which in turn is transcribed by the motility sigma factor SigD (FliA) (38–40). Multiple negative regulators can also repress *tcdR* transcription, thereby preventing toxin production (41, 42). We investigated the expression of the positive regulator of toxin transcription *sigD* to determine if its transcription was affected in the *CD1492* mutant. As shown in Fig. 7A, *sigD* expression is >6-fold lower in the *CD1492* mutant grown on sporulation agar. A corresponding decrease in *fliC* transcription, which is SigD dependent, was also observed in the *CD1492* mutant, indicating that SigD activity is also reduced. Decreased SigD activity is known to dramatically lower *tcdA* and *tcdB* expression, as well as flagellum production and motility (20, 39, 40). Accordingly, we compared the swimming motility of the *CD1492* mutant to that of the parent strain on soft agar medium (Fig. 7B) but observed no significant difference in motility *in vitro*. However, examination of *C. difficile fliC* transcription from the ceca of infected animals revealed lower *fliC* expression in hamsters infected with the *CD1492* mutant, demonstrating that SigD activity is decreased *in vivo* (Fig. 7C). The timing and expression of *sigD* and flagellar genes during infection affect colonization by and the virulence of *C. difficile* and other motile pathogens and thus probably contribute to the decreased virulence of the *CD1492* mutant in the animal model (43–47).

The specific factors that control *sigD* transcription and activity have not been fully elucidated for *C. difficile in vitro*, and even less is known about the regulation of SigD *in vivo*. A few negative regulators of SigD have been identified, including the early sporulation effector RstA, the stationary-phase sigma factor SigH, and

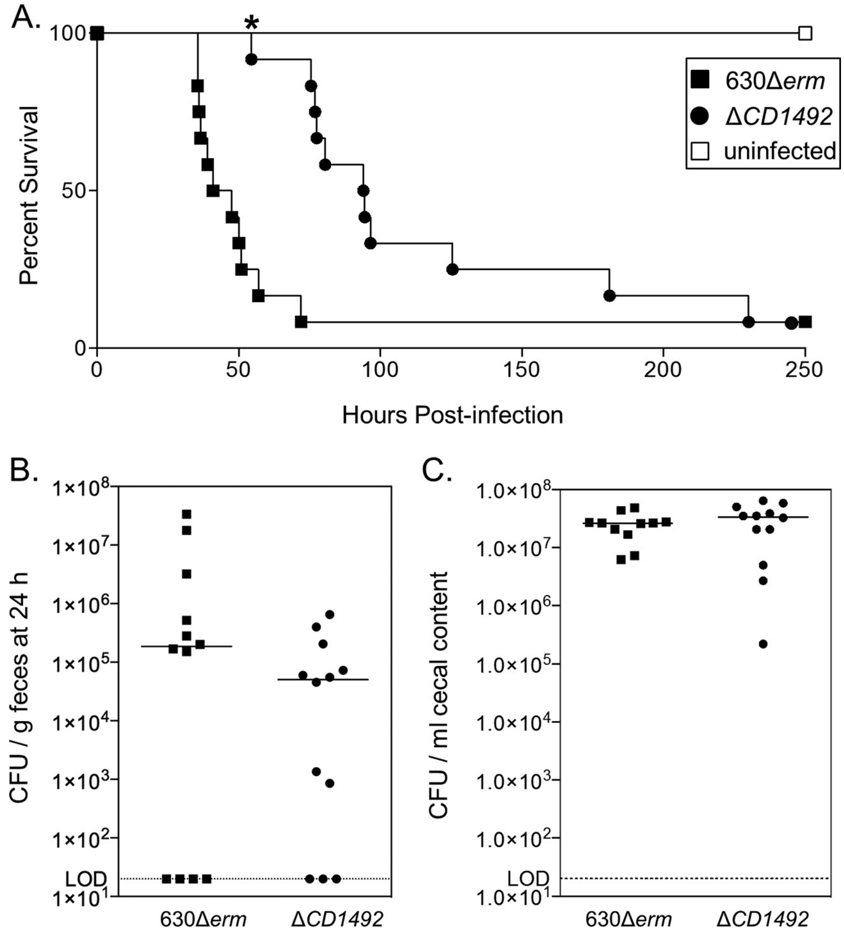

FIG 5 Deletion of *CD1492* results in decreased virulence in the hamster model of infection. (A) Kaplan-Meier survival plot of the survival times of Syrian golden hamsters infected with 5,000 spores of *C. difficile* strain 630Δ*erm* ($n = 12$) or MC674 (Δ*CD1492*; $n = 12$). The mean times to morbidity were as follows: 630Δ*erm*, 45.5 ± 3.5 h; Δ*CD1492*, 107.9 ± 52.5 h. ($P < 0.01$, log rank test). The total number of CFU of *C. difficile* recovered from feces at 24 h postinfection (B) or per milliliter of cecal content recovered postmortem (C) is shown. The solid lines in panels B and C represent the median CFU count of each strain, and the dotted lines denote the limit of detection (LOD; 2×10^1 CFU/g or CFU/ml). Statistical significance was assessed by one-way ANOVA. Animals infected with 630Δ*erm* served as positive infection controls that were shown in a parallel study (22).

the anti-sigma factor FlgM (24, 39, 48, 49). We examined the transcription of *rstA* on sporulation medium and found that its expression was more than 3-fold lower in the *CD1492* mutant than in the parent strain (Fig. 7A). This finding is intriguing, as an *rstA* null mutant has higher *sigD* expression and, accordingly, RstA negatively affects *sigD* transcription (24). Further investigation of the expression profiles for the *CD1492* and *rstA* mutants revealed that the gene expression and sporulation profiles of these mutants are reversed (Table 4). The inverse correlation of gene expression and phenotypes between the *rstA* and *CD1492* mutants strongly suggests that the activities of these factors are linked within a regulatory pathway, likely with CD1492 functioning upstream of RstA. Although it is possible that CD1492 acts directly on Spo0A as a phosphatase, the effects of CD1492 on *sigD* and *rstA* expression suggest that CD1492 functions at least partially independently of Spo0A (10).

DISCUSSION

The formation of endospores is critical for the survival of *C. difficile* outside the host and for dissemination of the bacterium to new hosts (50). The basic morphological programs for producing a dormant spore are similar in *C. difficile* and well-characterized spore formers such as *Bacillus subtilis*, but the specific factors that regulate entry into sporulation are not well conserved (5, 10, 16, 31, 51, 52). The specific signals that activate sporulation are not known, but it is anticipated that, like other sporulating members of the phylum *Firmicutes*, the sporulation-initiating and -inhibiting signals for *C. difficile* are transmitted through predicted sporulation sensor histidine kinases, including CD1492. Our investigation found that the predicted sporulation kinase CD1492 inhibits sporulation initiation. Moreover, CD1492 affects the function of factors other than its anticipated target, Spo0A, including the expression of the sporulation regulator RstA and the motility and toxin regulator SigD. As a result, CD1492 impacts both sporulation and motility during the infection of a host.

In the spore-forming members of the phylum *Firmicutes*, the master regulator of sporulation Spo0A is activated by phosphorylation and inactivated by dephosphorylation (16, 53). In the sporulating anaerobes that have been studied, most of the predicted orphan kinases that affect sporulation initiation function as Spo0A activators (34, 35). Mutation of the catalytic histidine

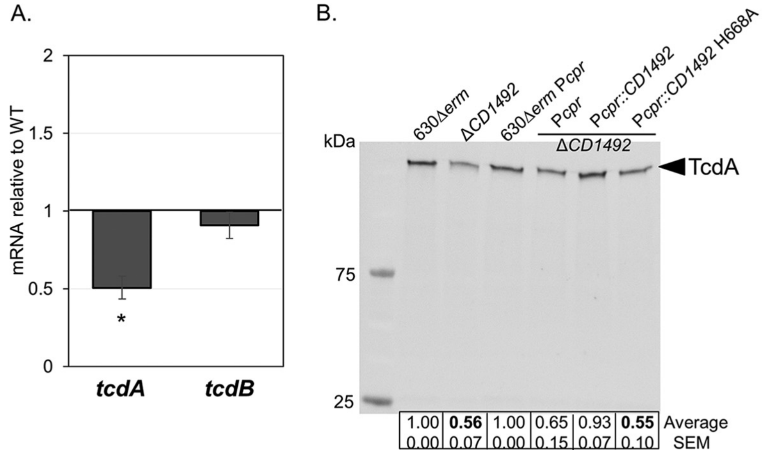

FIG 6 Toxin production in the Δ*CD1492* mutant. (A) Transcriptional analysis of the primary toxins, *tcdA* and *tcdB* in the Δ*CD1492* mutant (MC674) relative to the parent strain, 630Δ*erm*. Cultures were grown on 70:30 agar medium for 12 h, RNA was harvested, cDNA was prepared, and qRT-PCR was performed with gene-specific primers as outlined in Materials and Methods. WT, wild type. (B) A representative Western blot analysis of TcdA in 630Δ*erm*, Δ*CD1492* (MC674), 630Δ*erm* p*Pcpr* (MC282, vector control), Δ*CD1492* p*Pcpr* (MC729, vector control), Δ*CD1492* p*PcprA*::*CD1492* (MC730), and Δ*CD1492* p*PcprA*::*CD1492*-H668A (MC771) grown in TY medium for 24 h. The mean values and the standard errors of the means of three independent experiments are shown at the bottom; bold values are statistically significantly different from those of the parent strain by a two-tailed Student *t* test or by a one-way ANOVA, followed by Dunnett's multiple-comparison test, as described in Materials and Methods. (C) qRT-PCR analysis of *tcdA* and *tcdB* transcript levels in cecal contents of hamsters infected with 630Δ*erm* ($n = 5$) or MC674 (Δ*CD1492*; $n = 5$). The mean values and the standard errors of the means are shown (*, $P \leq 0.05$ by two-tailed Student *t* test).

residue in CD1492 resulted in a loss of activity and failure to restore the mutant phenotype (*CD1492* p*PcprA*::*CD1492*-H668A, MC771). Therefore, CD1492 may function as a kinase on a target other than Spo0A but more likely acts as a phosphatase on Spo0A. In addition to CD1492 of *C. difficile*, other predicted sensor kinases were found to negatively impact sporulation in two anaerobic species, *Clostridium acetobutylicum* and "*Ruminiclostridium* (formerly *Clostridium*) *thermocellum*." In *C. acetobutylicum*, the predicted kinase Ca_C0437 represses sporulation and can catalyze ATP-dependent dephosphorylation of Spo0A~P *in vitro* (35) (see Fig. S5 in the supplemental material). *In vitro* phosphotransfer data suggest that Ca_C0437 acts as a phosphatase, playing a role similar to that of the Spo0E and Rap proteins that inactivate Spo0A in *B. subtilis* (54, 55). A similar sporulation histidine kinase-like protein, Clo1313_1973, was identified in "*R. thermocellum*" (34) (see Fig. S5). The role of these histidine kinase-like phosphatases in preventing initiation is further evidence that the anaerobic spore formers evolved strategies that are distinct from the *Bacillus* model but still achieve the same goal of Spo0A inactivation.

In *C. acetobutylicum*, three positive-acting and one negative-acting sporulation kinase-like proteins have been identified, while in "*R. thermocellum*," four positive regulators and one negative regulator were found (34, 35) (see Fig. S5). Analysis of these sporulation sensor mutants uncovered the existence of two genetic pathways that can lead to activation of sporulation in each of these species (34, 35). *C. difficile* has three putative sporulation histidine kinase-like proteins: CD1492 and CD2492, which are predicted

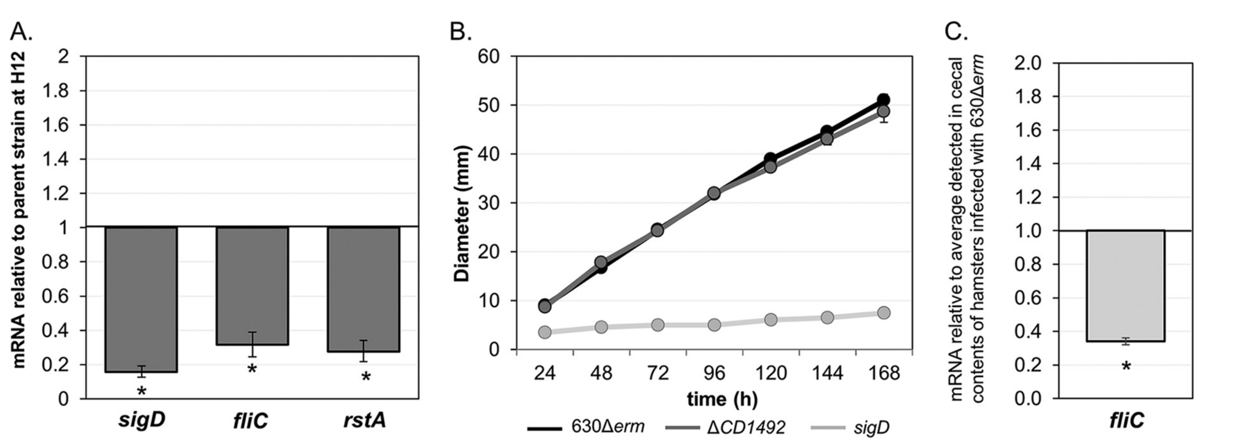

FIG 7 The Δ*CD1492* mutant has decreased expression of toxin, motility, and sporulation regulators. (A) qRT-PCR analysis of the motility and toxin-associated sigma factor *sigD*, the *sigD*-dependent gene *fliC*, and the sporulation and *sigD* regulator *rstA* in the Δ*CD1492* mutant relative to those in parent strain 630Δ*erm*. Cultures were grown on 70:30 agar medium for 12 h, RNA was harvested, cDNA was prepared, and qPCR was performed with gene-specific primers as outlined in Materials and Methods. (B) Motility of 630Δ*erm*, Δ*CD1492* (MC674), and *sigD* (RT1075, negative control) mutant strains in one-half-concentration BHI medium with 0.3% agar. Swimming diameters were measured every 24 h for a total of 168 h. (C) qRT-PCR analysis of *fliC* transcript levels in the cecal contents of hamsters infected with 630Δ*erm* ($n = 5$) or MC674 (Δ*CD1492*; $n = 5$). The mean values and the standard errors of the means are shown (*, $P \leq 0.05$ by two-tailed Student *t* test).

TABLE 4 Comparison of gene expression and phenotypes of *rstA* and *CD1492* null mutants

Trait	Product	Fold change[f] vs parent	
		CD1492	*rstA*[a]
Phenotype[b]			
Sporulation frequency[c]		↑ **2.4**	↓ **20.1**
Virulence[d]		↓ **2.4**	↑ **1.3**
Gene expression[b]			
CD2492	Sporulation sensor kinase	↓ 1.2	↑ **2.4**
CD1579	Sporulation sensor kinase	↓ **1.9**	↑ **4.9**
CD1492	Sporulation sensor kinase	—[e]	↑ **2.4**
rstA	Sporulation/*sigD* regulator	↓ **3.6**	—[e]
spo0A	Sporulation master regulator	↑ 1.9	↓ 1.4
sigF	Sporulation sigma factor	↑ **2.9**	↓ **2.2**
sigE	Sporulation sigma factor	↑ **2.3**	↓ **6.4**
sigD	Motility sigma factor	↓ **6.3**	↑ **2.5**
fliC	Flagellar component	↓ **3.1**	↑ **3.5**
tcdR	Toxin sigma factor	0.0	↑ **2.9**
tcdA	Toxin A	↓ **2.0**	↑ **4.0**
tcdB	Toxin B	↓ 1.1	↑ **3.5**

[a] *rstA* values obtained under the same experimental conditions, previously reported (24).
[b] All mean fold changes reported are relative to parent strain 630Δ*erm*. Bold values are statistically significantly different ($P \leq 0.05$ by two-tailed Student *t* test).
[c] As determined by phase-contrast microscopy.
[d] Defined here as fold change in time to morbidity in hamsters.
[e] No significant transcript levels were detected in null mutants.
[f] Ratios of the mean relative transcript levels for mutant and wild-type strains.

membrane proteins, and CD1579, which is likely cytosolic (11) (Fig. 1). Comparing the sporulation sensors of *C. difficile*, "*R. thermocellum*," and *C. acetobutylicum* (smart.embl-heidelberg.de); (56, 57), there is tremendous variability in sensor architecture and there are no known or apparent structural features that are predictive of the role these factors play in the initiation cascade (Fig. 1; see Fig. S5). BLAST analysis also revealed that orthologs of CD1492 are encoded in closely related species such as *C. sordellii*, "*C. dakarense*," and *C. mangenotii*, but these factors have not been characterized. On the basis of the protein structures and what is known about the initiation pathways, it appears that each species evolved independent means of processing the signals that stimulate or inhibit sporulation, which is expected since these distant relatives inhabit very different ecological niches.

The phosphatase functions of sensor kinases are known to contribute to the activation state of their cognate response regulators (58–60). The roles of Ca_C0437, Clo1313_1973, and CD1492 as phosphatases are supported by the hypersporulation phenotypes observed in the respective null mutants, though the mechanisms of phosphatase activity have not been characterized. Traditionally, the specific functions of sporulation phosphotransfer proteins have been examined through *in vitro* phosphotransfer assays, which demonstrate the ability of potential interacting partners to give or receive phosphate (11, 14, 35, 61, 62). While *in vitro* phosphotransfer assays can demonstrate interactions between individual sporulation initiation factors, phosphotransfer between these proteins often occurs in both directions *in vitro*, whereas *in vivo*, one direction of transfer is favored (14, 32). Consequently, the results of these assays are often not reliable indicators of the direction of transfer or the order of pathway components. However, a combination of phosphotransfer assays, genetic analyses, overexpression phenotypes, and characterization of multiple null mutants in pathway components can help unravel the roles of individual factors, which we plan to perform in future studies (32, 34).

In addition to defining the specific role of CD1492 in Spo0A activation, determining how CD1492 affects RstA and SigD will help to reveal how these factors interact to control both sporulation and pathogenesis. Previous studies of sporulation-defective *spo0A* and *rstA* mutants have observed different effects on virulence and have revealed indirect links between sporulation and pathogenesis (12, 24, 63, 64). Although the spore-forming anaerobes are currently thought to have a simplified mechanism for initiating sporulation, the discovery of interactions between regulators of initiation, toxin production, and motility indicates that the initiation process in these species is far from simple. The data suggest that there are multiple layers of transcriptional and post-translational regulation, as well as protein-protein interactions that control these processes. Further defining the complex genetic pathways, the protein interactions and the signals that activate sporulation in *C. difficile* could provide clues about how to manipulate this process and prevent the spread of disease.

ACKNOWLEDGMENTS

We give special thanks to Charles Moran and members of the McBride lab for helpful suggestions and discussions during the course of this work. In addition, we thank Gregory Tharp, Nirav Patel, and Steven Bosinger of the Yerkes Genomics Core Laboratory for assistance with the next-generation sequencing experiments and data analysis.

The Genomics Core receives financial support from P51 OD011132 (Support of the Yerkes National Primate Research Center). This research was supported by the U.S. National Institutes of Health through research grants DK087763, DK101870, AI109526, and AI116933 to S.M.M.; T32 GM008169 to E.C.W.; and T32 AI106699 to K.L.N. and S.E.A.

The content of this report is solely the responsibility of the authors and does not necessarily reflect the official views of the National Institutes of Health.

FUNDING INFORMATION

This work, including the efforts of Shonna M. McBride, was funded by HHS | NIH | National Institute of Allergy and Infectious Diseases (NIAID) (AI109526). This work, including the efforts of Shonna M. McBride, was funded by HHS | NIH | National Institute of Allergy and Infectious Diseases (NIAID) (AI116933). This work, including the efforts of Kathryn L. Nawrocki and Sarah E. Anderson, was funded by HHS | NIH | National Institute of Allergy and Infectious Diseases (NIAID) (AI106699). This work, including the efforts of Emily C. Woods, was funded by HHS | NIH | National Institute of General Medical Sciences (NIGMS) (GM008169). This work, including the efforts of Shonna M. McBride, was funded by HHS | NIH | National Institute of Diabetes and Digestive and Kidney Diseases (NIDDK) (DK101870). This work, including the efforts of Shonna M. McBride, was funded by HHS | NIH | National Institute of Diabetes and Digestive and Kidney Diseases (NIDDK) (DK087763).

REFERENCES

1. **Wilson KH, Kennedy MJ, Fekety FR.** 1982. Use of sodium taurocholate to enhance spore recovery on a medium selective for *Clostridium difficile*. J Clin Microbiol **15:**443–446.
2. **Sorg JA, Sonenshein AL.** 2008. Bile salts and glycine as cogerminants for *Clostridium difficile* spores. J Bacteriol **190:**2505–2512. http://dx.doi.org/10.1128/JB.01765-07.
3. **Voth DE, Ballard JD.** 2005. *Clostridium difficile* toxins: mechanism of action and role in disease. Clin Microbiol Rev **18:**247–263. http://dx.doi.org/10.1128/CMR.18.2.247-263.2005.
4. **Theriot CM, Young VB.** 2015. Interactions between the gastrointestinal

microbiome and *Clostridium difficile*. Annu Rev Microbiol **69:**445–461. http://dx.doi.org/10.1146/annurev-micro-091014-104115.

5. **McBride SM.** 2014. More than one way to make a spore. Microbe **9:**153–157. http://dx.doi.org/10.1128/microbe.9.153.1.
6. **Koenigsknecht MJ, Theriot CM, Bergin IL, Schumacher CA, Schloss PD, Young VB.** 2015. Dynamics and establishment of *Clostridium difficile* infection in the murine gastrointestinal tract. Infect Immun **83:**934–941. http://dx.doi.org/10.1128/IAI.02768-14.
7. **Dubberke E.** 2012. Strategies for prevention of *Clostridium difficile* infection. J Hosp Med **7**(Suppl 3)**:**S14–S17. http://dx.doi.org/10.1002/jhm.1908.
8. **Vohra P, Poxton IR.** 2011. Efficacy of decontaminants and disinfectants against *Clostridium difficile*. J Med Microbiol **60:**1218–1224. http://dx.doi.org/10.1099/jmm.0.030288-0.
9. **Ali S, Moore G, Wilson AP.** 2011. Spread and persistence of *Clostridium difficile* spores during and after cleaning with sporicidal disinfectants. J Hosp Infect **79:**97–98. http://dx.doi.org/10.1016/j.jhin.2011.06.010.
10. **Fimlaid KA, Bond JP, Schutz KC, Putnam EE, Leung JM, Lawley TD, Shen A.** 2013. Global analysis of the sporulation pathway of *Clostridium difficile*. PLoS Genet **9:**e1003660. http://dx.doi.org/10.1371/journal.pgen.1003660.
11. **Underwood S, Guan S, Vijayasubhash V, Baines SD, Graham L, Lewis RJ, Wilcox MH, Stephenson K.** 2009. Characterization of the sporulation initiation pathway of *Clostridium difficile* and its role in toxin production. J Bacteriol **191:**7296–7305. http://dx.doi.org/10.1128/JB.00882-09.
12. **Pettit LJ, Browne HP, Yu L, Smits WK, Fagan RP, Barquist L, Martin MJ, Goulding D, Duncan SH, Flint HJ, Dougan G, Choudhary JS, Lawley TD.** 2014. Functional genomics reveals that *Clostridium difficile* Spo0A coordinates sporulation, virulence and metabolism. BMC Genomics **15:**160. http://dx.doi.org/10.1186/1471-2164-15-160.
13. **Sonenshein AL.** 2000. Control of sporulation initiation in *Bacillus subtilis*. Curr Opin Microbiol **3:**561–566. http://dx.doi.org/10.1016/S1369-5274(00)00141-7.
14. **Burbulys D, Trach KA, Hoch JA.** 1991. Initiation of sporulation in *B. subtilis* is controlled by a multicomponent phosphorelay. Cell **64:**545–552. http://dx.doi.org/10.1016/0092-8674(91)90238-T.
15. **Hoch JA.** 2000. Two-component and phosphorelay signal transduction. Curr Opin Microbiol **3:**165–170. http://dx.doi.org/10.1016/S1369-5274(00)00070-9.
16. **Paredes CJ, Alsaker KV, Papoutsakis ET.** 2005. A comparative genomic view of clostridial sporulation and physiology. Nat Rev Microbiol **3:**969–978. http://dx.doi.org/10.1038/nrmicro1288.
17. **Edwards AN, Suárez JM, McBride SM.** 2013. Culturing and maintaining *Clostridium difficile* in an anaerobic environment. J Vis Exp **79:**e50787. http://dx.doi.org/10.3791/50787:e50787.
18. **Smith CJ, Markowitz SM, Macrina FL.** 1981. Transferable tetracycline resistance in *Clostridium difficile*. Antimicrob Agents Chemother **19:**997–1003. http://dx.doi.org/10.1128/AAC.19.6.997.
19. **Luria SE, Burrous JW.** 1957. Hybridization between *Escherichia coli* and *Shigella*. J Bacteriol **74:**461–476.
20. **Purcell EB, McKee RW, McBride SM, Waters CM, Tamayo R.** 2012. Cyclic diguanylate inversely regulates motility and aggregation in *Clostridium difficile*. J Bacteriol **194:**3307–3316. http://dx.doi.org/10.1128/JB.00100-12.
21. **Sorg JA, Dineen SS.** 2009. Laboratory maintenance of *Clostridium difficile*. Curr Protoc Microbiol **Chapter 9:**Unit9A.1. http://dx.doi.org/10.1002/9780471729259.mc09a01s12.
22. **McBride SM, Sonenshein AL.** 2011. The *dlt* operon confers resistance to cationic antimicrobial peptides in *Clostridium difficile*. Microbiology **157:**1457–1465. http://dx.doi.org/10.1099/mic.0.045997-0.
23. **Bouillaut L, McBride SM, Sorg JA.** 2011. Genetic manipulation of *Clostridium difficile*. Curr Protoc Microbiol **Chapter 9:**Unit 9A.2. http://dx.doi.org/10.1002/9780471729259.mc09a02s20.
24. **Edwards AN, Tamayo R, McBride SM.** 2016. A novel regulator controls *Clostridium difficile* sporulation, motility and toxin production. Mol Microbiol **100:**954–971. http://dx.doi.org/10.1111/mmi.13361.
25. **Harju S, Fedosyuk H, Peterson KR.** 2004. Rapid isolation of yeast genomic DNA: bust n' grab. BMC Biotechnol **4:**8. http://dx.doi.org/10.1186/1472-6750-4-8.
26. **Cartman ST, Kelly ML, Heeg D, Heap JT, Minton NP.** 2012. Precise manipulation of the *Clostridium difficile* chromosome reveals a lack of association between the *tcdC* genotype and toxin production. Appl Environ Microbiol **78:**4683–4690. http://dx.doi.org/10.1128/AEM.00249-12.
27. **Putnam EE, Nock AM, Lawley TD, Shen A.** 2013. SpoIVA and SipL are *Clostridium difficile* spore morphogenetic proteins. J Bacteriol **195:**1214–1225. http://dx.doi.org/10.1128/JB.02181-12.
28. **Edwards AN, Nawrocki KL, McBride SM.** 2014. Conserved oligopeptide permeases modulate sporulation initiation in *Clostridium difficile*. Infect Immun **82:**4276–4291. http://dx.doi.org/10.1128/IAI.02323-14.
29. **Dineen SS, McBride SM, Sonenshein AL.** 2010. Integration of metabolism and virulence by *Clostridium difficile* CodY. J Bacteriol **192:**5350–5362. http://dx.doi.org/10.1128/JB.00341-10.
30. **Schmittgen TD, Livak KJ.** 2008. Analyzing real-time PCR data by the comparative C(T) method. Nat Protoc **3:**1101–1108. http://dx.doi.org/10.1038/nprot.2008.73.
31. **Pereira FC, Saujet L, Tome AR, Serrano M, Monot M, Couture-Tosi E, Martin-Verstraete I, Dupuy B, Henriques AO.** 2013. The spore differentiation pathway in the enteric pathogen *Clostridium difficile*. PLoS Genet **9:**e1003782. http://dx.doi.org/10.1371/journal.pgen.1003782.
32. **Jiang M, Shao W, Perego M, Hoch JA.** 2000. Multiple histidine kinases regulate entry into stationary phase and sporulation in *Bacillus subtilis*. Mol Microbiol **38:**535–542. http://dx.doi.org/10.1046/j.1365-2958.2000.02148.x.
33. **Perego M, Cole SP, Burbulys D, Trach K, Hoch JA.** 1989. Characterization of the gene for a protein kinase which phosphorylates the sporulation-regulatory proteins Spo0A and Spo0F of *Bacillus subtilis*. J Bacteriol **171:**6187–6196.
34. **Mearls EB, Lynd LR.** 2014. The identification of four histidine kinases that influence sporulation in. Clostridium thermocellum. Anaerobe **28:**109–119. http://dx.doi.org/10.1016/j.anaerobe.2014.06.004.
35. **Steiner E, Dago AE, Young DI, Heap JT, Minton NP, Hoch JA, Young M.** 2011. Multiple orphan histidine kinases interact directly with Spo0A to control the initiation of endospore formation in. Clostridium acetobutylicum. Mol Microbiol **80:**641–654. http://dx.doi.org/10.1111/j.1365-2958.2011.07608.x.
36. **Suárez JM, Edwards AN, McBride SM.** 2013. The *Clostridium difficile cpr* locus is regulated by a noncontiguous two-component system in response to type A and B lantibiotics. J Bacteriol **195:**2621–2631. http://dx.doi.org/10.1128/JB.00166-13.
37. **Bouillaut L, Dubois T, Sonenshein AL, Dupuy B.** 2015. Integration of metabolism and virulence in *Clostridium difficile*. Res Microbiol **166:**375–383. http://dx.doi.org/10.1016/j.resmic.2014.10.002.
38. **Mani N, Dupuy B.** 2001. Regulation of toxin synthesis in *Clostridium difficile* by an alternative RNA polymerase sigma factor. Proc Natl Acad Sci U S A **98:**5844–5849. http://dx.doi.org/10.1073/pnas.101126598.
39. **El Meouche I, Peltier J, Monot M, Soutourina O, Pestel-Caron M, Dupuy B, Pons JL.** 2013. Characterization of the SigD regulon of *C. difficile* and its positive control of toxin production through the regulation of *tcdR*. PLoS One **8:**e83748. http://dx.doi.org/10.1371/journal.pone.0083748.
40. **McKee RW, Mangalea MR, Purcell EB, Borchardt EK, Tamayo R.** 2013. The second messenger cyclic di-GMP regulates *Clostridium difficile* toxin production by controlling expression of *sigD*. J Bacteriol **195:**5174–5185. http://dx.doi.org/10.1128/JB.00501-13.
41. **Antunes A, Martin-Verstraete I, Dupuy B.** 2011. CcpA-mediated repression of *Clostridium difficile* toxin gene expression. Mol Microbiol **79:**882–899. http://dx.doi.org/10.1111/j.1365-2958.2010.07495.x.
42. **Dineen SS, Villapakkam AC, Nordman JT, Sonenshein AL.** 2007. Repression of *Clostridium difficile* toxin gene expression by CodY. Mol Microbiol **66:**206–219. http://dx.doi.org/10.1111/j.1365-2958.2007.05906.x.
43. **Aubry A, Hussack G, Chen W, KuoLee R, Twine SM, Fulton KM, Foote S, Carrillo CD, Tanha J, Logan SM.** 2012. Modulation of toxin production by the flagellar regulon in *Clostridium difficile*. Infect Immun **80:**3521–3532. http://dx.doi.org/10.1128/IAI.00224-12.
44. **Scaria J, Janvilisri T, Fubini S, Gleed RD, McDonough SP, Chang YF.** 2011. *Clostridium difficile* transcriptome analysis using pig ligated loop model reveals modulation of pathways not modulated in vitro. J Infect Dis **203:**1613–1620. http://dx.doi.org/10.1093/infdis/jir112.
45. **Dingle TC, Mulvey GL, Armstrong GD.** 2011. Mutagenic analysis of the *Clostridium difficile* flagellar proteins, FliC and FliD, and their contribution to virulence in hamsters. Infect Immun **79:**4061–4067. http://dx.doi.org/10.1128/IAI.05305-11.
46. **Baban ST, Kuehne SA, Barketi-Klai A, Cartman ST, Kelly ML, Hardie KR, Kansau I, Collignon A, Minton NP.** 2013. The role of flagella in *Clostridium difficile* pathogenesis: comparison between a non-epidemic

and an epidemic strain. PLoS One **8:**e73026. http://dx.doi.org/10.1371/journal.pone.0073026.
47. **Janoir C.** 2016. Virulence factors of *Clostridium difficile* and their role during infection. Anaerobe **37:**13–24. http://dx.doi.org/10.1016/j.anaerobe.2015.10.009.
48. **Janoir C, Deneve C, Bouttier S, Barbut F, Hoys S, Caleechum L, Chapeton-Montes D, Pereira FC, Henriques AO, Collignon A, Monot M, Dupuy B.** 2013. Adaptive strategies and pathogenesis of *Clostridium difficile* from in vivo transcriptomics. Infect Immun **81:**3757–3769. http://dx.doi.org/10.1128/IAI.00515-13.
49. **Saujet L, Monot M, Dupuy B, Soutourina O, Martin-Verstraete I.** 2011. The key sigma factor of transition phase, SigH, controls sporulation, metabolism, and virulence factor expression in *Clostridium difficile*. J Bacteriol **193:**3186–3196. http://dx.doi.org/10.1128/JB.00272-11.
50. **Deakin LJ, Clare S, Fagan RP, Dawson LF, Pickard DJ, West MR, Wren BW, Fairweather NF, Dougan G, Lawley TD.** 2012. The *Clostridium difficile spo0A* gene is a persistence and transmission factor. Infect Immun **80:**2704–2711. http://dx.doi.org/10.1128/IAI.00147-12.
51. **Saujet L, Pereira FC, Serrano M, Soutourina O, Monot M, Shelyakin PV, Gelfand MS, Dupuy B, Henriques AO, Martin-Verstraete I.** 2013. Genome-wide analysis of cell type-specific gene transcription during spore formation in *Clostridium difficile*. PLoS Genet **9:**e1003756. http://dx.doi.org/10.1371/journal.pgen.1003756.
52. **Edwards AN, McBride SM.** 2014. Initiation of sporulation in *Clostridium difficile*: a twist on the classic model. FEMS Microbiol Lett **358:**110–118. http://dx.doi.org/10.1111/1574-6968.12499.
53. **Brown DP, Ganova-Raeva L, Green BD, Wilkinson SR, Young M, Youngman P.** 1994. Characterization of *spo0A* homologues in diverse *Bacillus* and *Clostridium* species identifies a probable DNA-binding domain. Mol Microbiol **14:**411–426. http://dx.doi.org/10.1111/j.1365-2958.1994.tb02176.x.
54. **Perego M, Hoch JA.** 1991. Negative regulation of *Bacillus subtilis* sporulation by the *spo0E* gene product. J Bacteriol **173:**2514–2520.
55. **Perego M.** 2001. A new family of aspartyl phosphate phosphatases targeting the sporulation transcription factor Spo0A of Bacillus subtilis. Mol Microbiol **42:**133–143.
56. **Schultz J, Milpetz F, Bork P, Ponting CP.** 1998. SMART, a simple modular architecture research tool: identification of signaling domains. Proc Natl Acad Sci U S A **95:**5857–5864. http://dx.doi.org/10.1073/pnas.95.11.5857.
57. **Letunic I, Doerks T, Bork P.** 2015. SMART: recent updates, new developments and status in 2015. Nucleic Acids Res **43:**D257–260. http://dx.doi.org/10.1093/nar/gku949.
58. **Kenney LJ.** 2010. How important is the phosphatase activity of sensor kinases? Curr Opin Microbiol **13:**168–176. http://dx.doi.org/10.1016/j.mib.2010.01.013.
59. **Raivio TL, Silhavy TJ.** 1997. Transduction of envelope stress in *Escherichia coli* by the Cpx two-component system. J Bacteriol **179:**7724–7733.
60. **De Wulf P, Lin EC.** 2000. Cpx two-component signal transduction in *Escherichia coli*: excessive CpxR-P levels underlie CpxA* phenotypes. J Bacteriol **182:**1423–1426. http://dx.doi.org/10.1128/JB.182.5.1423-1426.2000.
61. **Stephenson K, Hoch JA.** 2002. Evolution of signalling in the sporulation phosphorelay. Mol Microbiol **46:**297–304. http://dx.doi.org/10.1046/j.1365-2958.2002.03186.x.
62. **Skerker JM, Perchuk BS, Siryaporn A, Lubin EA, Ashenberg O, Goulian M, Laub MT.** 2008. Rewiring the specificity of two-component signal transduction systems. Cell **133:**1043–1054. http://dx.doi.org/10.1016/j.cell.2008.04.040.
63. **Mackin KE, Carter GP, Howarth P, Rood JI, Lyras D.** 2013. Spo0A differentially regulates toxin production in evolutionarily diverse strains of *Clostridium difficile*. PLoS One **8:**e79666. http://dx.doi.org/10.1371/journal.pone.0079666.
64. **Rosenbusch KE, Bakker D, Kuijper EJ, Smits WK.** 2012. *C. difficile* 630Δ*erm* Spo0A regulates sporulation, but does not contribute to toxin production, by direct high-affinity binding to target DNA. PLoS One **7:**e48608. http://dx.doi.org/10.1371/journal.pone.0048608.
65. **Wüst J, Hardegger U.** 1983. Transferable resistance to clindamycin, erythromycin, and tetracycline in *Clostridium difficile*. Antimicrob Agents Chemother **23:**784–786. http://dx.doi.org/10.1128/AAC.23.5.784.
66. **Hussain HA, Roberts AP, Mullany P.** 2005. Generation of an erythromycin-sensitive derivative of *Clostridium difficile* strain 630 (630Deltaerm) and demonstration that the conjugative transposon Tn916DeltaE enters the genome of this strain at multiple sites. J Med Microbiol **54:**137–141. http://dx.doi.org/10.1099/jmm.0.45790-0.
67. **Thomas CM, Smith CA.** 1987. Incompatibility group P plasmids: genetics, evolution, and use in genetic manipulation. Annu Rev Microbiol **41:**77–101. http://dx.doi.org/10.1146/annurev.mi.41.100187.000453.
68. **Yanisch-Perron C, Vieira J, Messing J.** 1985. Improved M13 phage cloning vectors and host strains: nucleotide sequences of the M13mp18 and pUC19 vectors. Gene **33:**103–119. http://dx.doi.org/10.1016/0378-1119(85)90120-9.
69. **McBride SM, Sonenshein AL.** 2011. Identification of a genetic locus responsible for antimicrobial peptide resistance in *Clostridium difficile*. Infect Immun **79:**167–176. http://dx.doi.org/10.1128/IAI.00731-10.